Structure of TiO_2-ZrO_2-SiO_2 xerogels from ^{13}C, ^{29}Si, ^{17}O and ^{1}H MAS NMR

Disusun oleh:
Philips Nicolas Gunawidjaja

FAKULTAS MATEMATIKA DAN ILMU PENGETAHUAN ALAM
UNIVERSITAS KATOLIK PARAHYANGAN
BANDUNG
2007

Abstract

A combination of ^{13}C, ^{29}Si, ^{17}O and ^{1}H NMR spectroscopy has been used to study the atomic structure of $(TiO_2)_x(ZiO_2)_y(SiO_2)_{1-x-y}$ xerogels, prepared by reacting partially-hydrolysed tetraethyl orthosilicate with Zirconium (IV) n-propoxide and Titanium (IV) butoxide. The extent of condensation of the silica network, based on the ^{29}Si MAS NMR results were found to be similar in most xerogels. Evidence of Si-O-M bonds (M = Ti, Zr) was clearly demonstrated in the ^{17}O NMR spectra of both $(TiO_2)_{0.05}(ZrO_2)_{0.15}(SiO_2)_{0.80}$ and $(TiO_2)_{0.15}(ZrO_2)_{0.05}(SiO_2)_{0.80}$ ^{17}O-enriched samples. Phase separation of Ti-O-Ti, Zr-O-Zr, and possibly Ti-O-Zr was observed after heat treatment at 750 °C. Finally, both ^{13}C and ^{1}H NMR show that heat treatment caused the removal of organics and OH groups from the network.

Content

1. Introduction

Mixed titania-zirconia-silica, $(TiO_2)_x(ZiO_2)_y(SiO_2)_{1-x-y}$, materials have attracted interest because of their technologically useful properties [1,2]. Silica glasses with a few mol% TiO_2, for example, can be used as ultra-low thermal expansion (ULE) glasses [3] and mixed zirconia-silica materials are used as coatings [4], fibres, catalysts [5] and high-refractive index glasses. In the optical industry [6], they can be produced as anti-reflective thin film coatings with tailored refractive indices. The properties of titania-zirconia-silica ternaries, however, are strongly dependent on their chemical composition, homogeneity and texture. Sol-gel processing, based on hydrolysis of metal alkoxide precursors, and subsequent condensation, offers a technique that combines atomic level mixing with a high degree of porosity without the need for very high processing temperature. Ti, Zr and Si alkoxides have very different hydrolysis rates that can mean phase separation occurs as Ti-rich, Zr-rich, and Si-rich region form. ^{17}O NMR has confirmed that atomic mixing can be achieved in SiO_2/TiO_2 glasses and SiO_2/ZrO_2 xerogels by revealing the presence of Ti-O-Si [7,8] or Zr-O-Si [9] bonds; in contrast, OTi_3 and OTi_4 features in the NMR spectra of glasses with higher TiO_2 content (~41 mol%) and different preparation conditions indicate that they are phase separated [10].

Although much work exists on the sol-gel process, details of the atomic-scale structure remains elusive; this problem may usefully be addressed using advanced spectroscopic and scattering techniques. Silica, titania-silica and zirconia-silica binaries have been studied in their crystalline phases using X-ray diffraction [11, 12], but relatively little work has been undertaken on the gels in their amorphous state. In this project, the atomic structure of a series $(TiO_2)_x(ZrO_2)_y(SiO_2)_{1-x-y}$ xerogels of various compositions and thermal histories is studied using a comprehensive advanced methodology of NMR spectroscopy. Parallel studies on the same samples are being carried out at the University of Kent using X-ray diffraction, Neutron Scattering, FT-IR and UV-vis techniques.

Section 2 contains a brief explanation on the background theory of NMR covering the chemical shift interaction, dipolar interaction, quadrupolar interaction, magic angle spinning (MAS), cross polarisation (CP), an introduction to nuclei and sol-gel processing. A brief overview of experimental procedures is given in section 3. The results and data analysis is presented in section 4, followed by a discussion in section 5. Finally, future development and a brief conclusion are given in section 6 and 7 respectively.

2. Background Theory

A basic knowledge of NMR is essential to understand the science behind this project. It is important to understand both how the method works and how results are interpreted using NMR as an analysing tool. This section of work will underline some of the most important aspects of the theory, extracted

from an article written by E.R. Andrew [13], H. Eckert [14], J.J. Fitzgerald [15] and R.K. Harris [16] which form the basic background of NMR theory.

2.1 Theory of Nuclear Magnetic Resonance

Any nuclei containing an odd number of protons or neutrons or both possesses angular momentum, I, and consequently a magnetic moment μ:

$$\mu = \gamma \hbar \underline{I} \tag{1}$$

where γ is a gyromagnetic ratio of the nuclei. The quantisation laws for angular momentum states that any nuclei with nuclear spin-quantum number I has $2I+1$ states. In the presence of an externally applied magnetic field of magnitude B_0 these states become non-degenerate and due to the Zeeman interaction,

$$H_z = \mu . B_0 \tag{2}$$

which results in discerete energy levels

$$E_m = - m\gamma \hbar B \tag{3}$$

where B is the magnetic field experienced by the nuclei, it consists of the external field B_0 and internal components B_{int} ($<< B_0$), which arise from internal interactions of the nuclei with their surrounding environment, where

$$B = B_0 + B_{int} \tag{4}$$

Since these internal fields are related to the structure of the material, their evaluation is of central interest in NMR spectroscopy. To measure the energy differences between the magnetic spin states (and hence B_{int}), electromagnetic waves in the radio frequency region are applied, and the frequency at which transitions between the states occur, is measured. At resonance the condition:

$$\omega = \gamma B = \gamma (B_0 + B_{int}) \tag{5}$$

holds. Where $\omega = 2\pi \nu$, and ν is the frequency of the electromagnetic radiation at which absorption occurs.

In general, B_{int} arises from the composite effect of a number of physically distinct internal interaction mechanisms. The three most important are magnetic dipole dipole coupling, magnetic shielding, and for nuclei with spin quantum number >1/2, nuclear electric quadrupole coupling.

Therefore, the complete NMR Hamiltonian can be expressed as:

$$H = H_z + H_{cs} + H_d + H_q \tag{6}$$

The above expression can be used to measure two crucial observables in NMR spectroscopy the energy eigenvalues as measured by resonance frequencies and lineshapes, and relaxation times, reflecting the rates of transitions between different spin states.

The influence of H_{cs}, H_d, (and sometimes H_q) upon the Zeeman energy levels is assumed to be minor compared to that of H_Z (termed the high field limit) and hence can be readily calculated by first-order perturbation theory. All of the above interactions are anisotropic. Consequently, the energy correction terms arising from the perturbation calculation contain an angular dependence, specifying the orientation of a molecular axis system relative to the applied magnetic field direction.

In the following sub-section, the physical nature of these internal interactions will be discussed in more detail.

2.2. The Chemical Shift Interaction

The chemical shift interaction, can be described as the effect of magnetic electron-nucleus interactions, which affect the local field experienced by the nuclei and hence influencing their resonance frequencies. Four factors affecting the chemical shifts consist of diamagnetic shielding by closed electronic shells, paramagnetic deshielding by the angular momenta of admixed excited electronic states, shielding or deshielding effects from rapidly fluctuating paramagnetic electron spins, and shielding or deshielding effects due to conduction electrons at the Fermi edge ("Knight shift"). Although these contributions are physically distinct, they are inseparable in the experiment. The chemical shift Hamiltonian, describing the composite effect of these interactions can be written as:

$$H = I(1-\sigma)B_0 \tag{7}$$

where σ is an orientation-dependent tensor quantity.

In solution-state NMR spectroscopy, rapid molecular tumbling averages out this orientation dependence and produces a narrow line at a position known as the isotropic chemical shift (δ_{iso}), which reflects the average electronic environment of the nucleus (Figure 1a). In spectra of powdered solid samples, however, all orientations of a given site with respect to the B_0 field are present. When the local

symmetry is less than cubic, most of these orientations have slightly different resonance frequency. This leads to a broad lineshape known as a "powder pattern" from which the eigenvalues of the chemical-shielding tensor in its diagonal representation ($\sigma_{11}, \sigma_{22}, \sigma_{33}$) can be extracted (Figure 1b-c). The eigenvalues are referred to as the principal values of the chemical-shielding anisotropy (CSA), which can often be related with chemical bonding, next nearest neighbour effects and site symmetry.

2.3. The Dipole-Dipole Interaction

Another important interaction in solid state NMR is the magnetic dipole-dipole interaction which describes the effect of the local magnetic fields associated with the magnetic moments of surrounding nuclei. Two mechanistic contributions to this effect need to be considered: the "direct" (through-space) coupling and the "indirect" spin-spin coupling transmitted via polarisation of bonding electrons. For NMR spectra in solids, the first term is usually dominant. The corresponding Hamiltonian describing the interaction between two spins with gyromagnetic ratios γ_1 and γ_2 separated by internuclear distance r is given by:

$$H_d = \gamma_1 \gamma_2 \hbar r^{-3} \{A + B + C + D + E + F\}$$

$$A = (1 - 3\cos^2\theta) I_{z1} I_{z2}$$

$$B = \frac{-(1 - 3\cos^2\theta) [I_{+1}I_{-2} + I_{+2}I_{-1}]}{4}$$
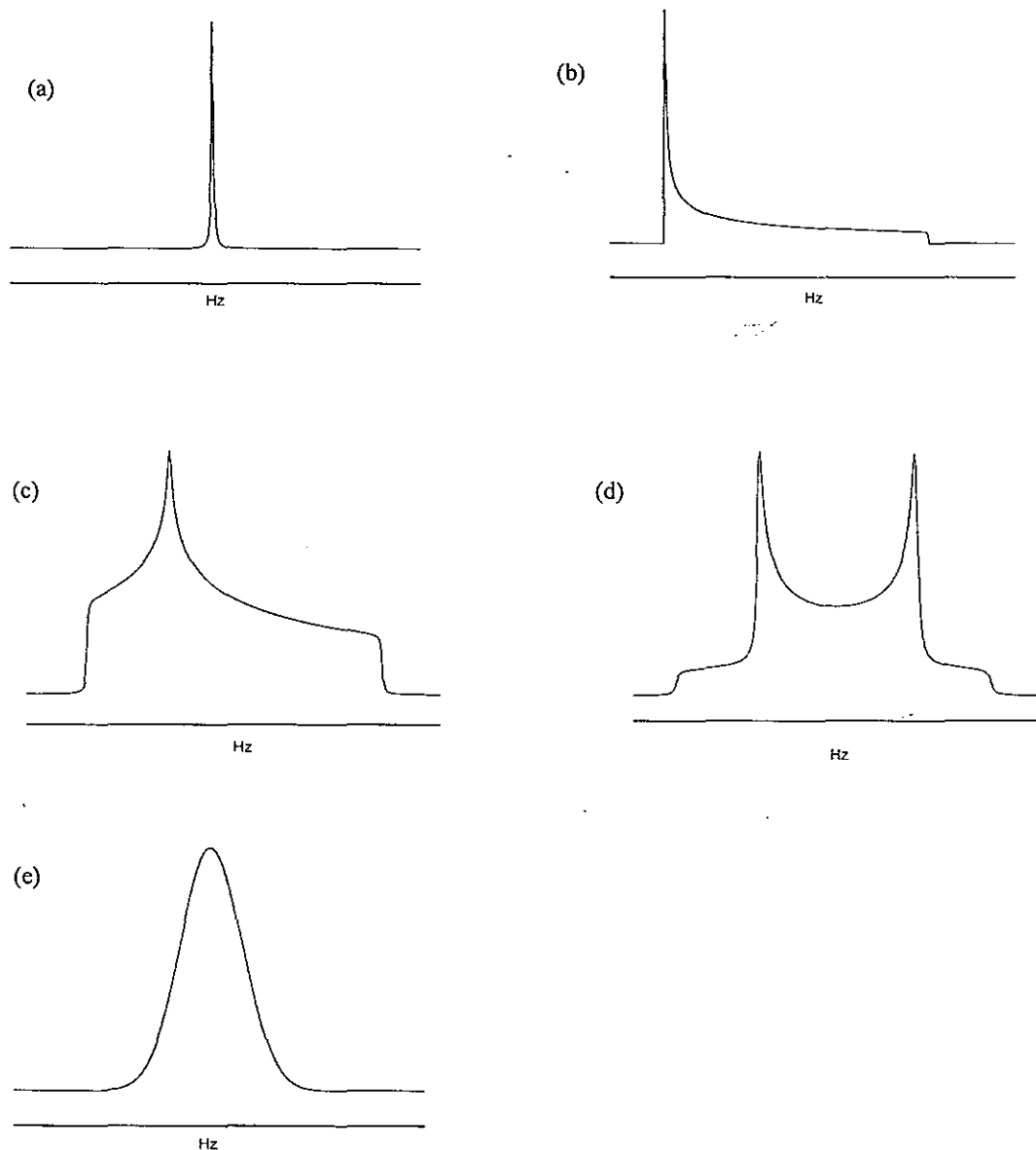
(8)

Fig. 1. Typical Chemical shift-dominated NMR powder patterns: (a) spherically symmetric chemical shift tensor, (b) axially symmetric chemical shift tensor, (c) asymmetric chemical shift tensor, (d) Dipolar Pake pattern for an isolated spin-pair, and (e) for many-spin system. Note that the principle values for CSA (σ_{11}, σ_{22}, σ_{33}) correspond to the 'singularities' in the powder spectra while the separation between the horns in the dipolar powder pattern is related to the internuclear distance [14, 15].

where terms A is a classical interaction of two magnetic moments and B is a flip-flop term describing the transition of the spins between spin-states, and term C to F have been omitted. H_d is proportional to r^{-3}, therefore provided this is the dominant interaction it can be used to determine bond-lengths.

As in the case of the chemical shift interaction, the direct dipolar interaction is anisotropic; it depends on the orientation of the internuclear vector with respect to the static B_0 field. Thus, for a powder sample, a broad lineshape will be generated. It is always axially symmetric as it is directed along the internucleaar vector. However, this pattern can contain singularities, which allow the determination of bond-length (Figure 1d-e)

2.4. The Nuclear Electric Quadrupole Interaction

The last perturbation on the nuclear magnetic energy levels which will be discussed, arises from the interaction of non-spherically symmetric nuclear charge distributions ("nuclear electric quadrupole tensor") with electric field gradient (EFG) generated by asymmetric charge distribution in molecules or lattice sites. The Hamiltonian characterising this interaction can be written as:

$$H_q = \frac{e^2qQ}{4I(2I-1)}[3I_z^2 - I^2 + \eta(I_x^2 + I_y^2)] \tag{9}$$

This interaction affects only nuclei with $I > \frac{1}{2}$ in non-cubic environments. The anisotropy of the EFG is described by a traceless symmetric tensor, which can be diagonalised to give the component eq_{xx}, eq_{yy}, and eq_{zz} in a principal axis system. Since according to the Laplace equation:

$$\sum_i eq_{ii} = 0 \tag{10}$$

only two principal components are independent. By convention, the quadrupolar interaction is then characterised by two parameters, e^2qQ/h and η. Here eQ is the scalar nuclear electric quadrupole moment, which expresses how much the nuclear charge distribution deviates from spherical symmetry; $eq(=eq_{zz})$ is the electric field gradient along the principal axis, and η, defined as $(eq_{xx}-eq_{yy})/eq_{zz}$. $(0 \#\eta \# 1)$, characterises the deviation of the electric field gradient from cylindrical symmetry.

Depending on its strength compared the Zeeman interaction, the effect of the nuclear quadrupolar interaction on the solid state NMR spectrum can be calculated using either first- or second-order perturbation theory. For half-integer spins, the central $\frac{1}{2}$ to $-\frac{1}{2}$ transition is, to first-order, unaffected by the quadrupole interaction. In principle, e^2qQ/h and η can be evaluated from the shapes of the satellite transitions, which give rise to powder pattern similar to those shown in Figure 1b and c, because they are governed by the same orientational dependence.

Stronger quadrupolar couplings neccesitate treatment by second-order perturbation theory. To second order, the lineshape of the central transition is affected. The second-order energy correction is inversely proportional to the nuclear magnetic resonance frequency, and exhibits a more complicated orientational dependence than the first order effect.

2.5. Magic Angle Spinning

Magic angle spinning (MAS) is a technique, which allows high-resolution spectra to be obtained from solid materials. This technique involves rotating the solid specimen about an axis inclined at the angle 54°44' to the direction of the magnetic field of the NMR magnet. This angle is $\cos^{-1} (1/\sqrt{3})$ and since several of the above interactions contain the term $(3 \cos^2\theta - 1)$ where θ is the angle between the applied magnetic field a direction r which depends on the interaction, sufficiently rapid rotation about this particular axis removes most broadening interactions from the NMR spectrum leaving only fine structure of the type which is found in NMR spectra of liquids.

2.6. ^{13}C Cross Polarisation

While magic angle spinning leads to line narrowing and thus increase sensitivity as well as resolution, cross polarisation can be used to further enhance the sensitivity of a nucleus with a low gyromagnetic ratio. [15, 17] Cross polarisation is a technique that is sensitive to heteronuclear dipolar coupling. This technique achieves magnetisation transfer from an abundant-spin system S (^{1}H) to the spin system of the observe-nucleus, I (^{13}C), whose signal is required. To accomplish this, the S-spins are first converted into a non-equilibrium state: a 90° preparation pulse followed by a strong B_1 field in phase with the transverse magnetisation which then forces the S-spins to precess around the B_1 direction ("spin-locking"). Since $B_1 \ll B_0$, the population difference between the energy states becomes significantly large, producing a driving force for energy exchange. The desired pathway in this technique involves magnetisation transfer via cross-relaxation to the I-spin system, i.e. the observe-nuclei. To this end, a radio frequency field is applied at the resonance of the I-spins such that:

$$(\omega_1)_{obs} = (\omega_1)_{ab....} \tag{11}$$

for a fixed amount of time t_m. This condition is known as the "Hartmann-Hahn condition" and ensures that the I-spins and the S-spins precess at the same frequency in the rotating frame. The rate of magnetisation transfer is characterised by the cross-relaxation time T_{cr}, which can be determined by

variable contact time experiments. The stronger the dipole coupling, the shorter the cross-relaxation time.

2.7. Introduction to Nuclei

^{29}Si is a spin ½ nucleus that has a low natural abundance of 4.7% (so active nuclei are well separated) and it is 2.1 times more sensitive than ^{13}C, but is usually characterised by long spin lattice relaxation times, T_1 [18, 19]. Hence, care must be taken to ensure that the pulse repetition time is not too fast and that the magnetisation had sufficient time to relax so that the proportion of different species remains quantitative. The ^{29}Si chemical shift is usually used to identify the type and connectivity of silicate species. The number of nearest neighbours (co-ordination number) has a large effect on δ whilst the connectivity to and type of nearest neighbours has a lesser but nevertheless is usually a measurable effect.

^{17}O is a spin 5/2 nucleus that has a very low natural abundance of 0.037% and low sensitivity compared to ^{13}C(6×10^{-2}). In addition, due to an efficient quadrupolar relaxation mechanism [16, 20], its T_1 values is usually very short. Since there is a difficulty in measuring the signal in its natural abundance, ^{17}O enriched water is normally used in the making of the samples. ^{17}O NMR can be very useful in characterising the chemical environment of oxygen in amorphous and disordered TiO_2-SiO_2 based materials. Indeed, oxygen-17 has been already been used to study the local structure of a variety of inorganic solids [21,22]. Its NMR parameters have been shown to be very sensitive to structure. Hence the co-ordination and bonding of oxygen can be distinguished through the ^{17}O isotropic chemical shift (δ_{iso}), which spans a large range $\approx$1500 ppm, and quadrupolar coupling parameters.

2.8 Sol-gel processing

Due to differences in reactivity toward hydrolysis and condensation reactions of the various precursors, sol-gel preparation of mixed oxides is usually quite delicate. Reactions occurring during sol-gel synthesis can be schematically written as follows:

$$M(OR)_n + mXOH \rightarrow [M(OR)_{n-m}(OX)_m] + mROH \qquad (12)$$
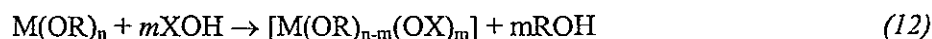
where X = H (hydrolysis) or M (condensation).

The first step of the reaction is usually a nucleophilic attack of OH groups on the metal M, which provokes an increase in metal co-ordination. Two parameters will thus control the reaction

kinetics: First the electronegativity of M and secondly, the ability of M to extend its co-ordination sphere.

These considerations justify the following classification for the reactivity of various alkoxides:

$$Si(OR)_4 \ll Ti(OR)_4 < Zr(OR)_4 \qquad (13)$$

$Si(OR)_4$ is by far the less reactive alkoxides, and a catalyst such as H^+ is used to increase their reactivity. On the contrary, the other two alkoxides are very reactive, and they usually lead to precipitation when hydrolysed. Chelating agents have often been used in sol-gel processing to decrease their reactivity. Specific acidic conditions can also decrease the reactivity [23].

Phase separation should be avoided for the preparation of mixed oxides such as the system being studied. The degree of homogeneity of the final materials will depend on the ability to favour co-condensation reactions between the pre-cursors, despite their intrinsic difference in reactivity. To compensate the difference in reactivity of the various alkoxides, Yoldas [24] proposed to prehydrolyze the silicon alkoxide under acidic conditions before addition of the titanium alkoxide. The idea is, in first stage, to consume the water in order to create a maximum number of Si-OH groups:

$$\equiv Si\text{-}OR + H_2O \rightarrow \equiv Si\text{-}OH + ROH \qquad (14)$$

In a second stage, the titanium alkoxide is added and will preferentially react with the silanol groups according to:

$$\equiv Si\text{-}OH + \equiv Ti\text{-}OR' \rightarrow \equiv Si\text{-}O\text{-}Ti \equiv + R'OH \qquad (15)$$
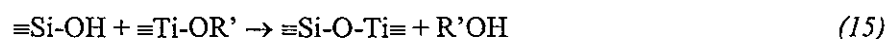
In a third stage, water is added to lead to gelation. Compared to other available method, this method is by far the most utilized ones.

3. Experimental details

3.1 Sample preparation

The samples were prepared using the sol-gel route from the following pre-cursors: tetraethyl orthosilicate, TEOS (Aldrich, 98%), Zirconium (IV) n-propoxide $Zr(OPr^n)_4$ (70 wt.% solution in propan-1-ol, Aldrich) and Titanium (IV) butoxide, $Ti(OPr_i)_4$ (Alfa, 99%). HCl (Fisons) was used as a catalyst to promote the hydrolysis and condensation reactions and ethanol was used as a mutual solvent.

Also, organic modifier acetylacetone (acac) was used to allow control of the reactivity of the Ti and Zr alkoxides by the formation of larger, slower reacting molecules by ligand exchange.

A modified method of Yoldas [24] was used to promote homogeneity within the mixed oxide samples. This involved prehydrolysis of the TEOS to maximise the number of Si-OH groups before mixing with the more reactive $Zr(OPr^n)_4$ and $Ti(OPr_i)_4$ precursors; the aim being to encourage Ti-O-Si and Zr-O-Si, bonding as opposed to Ti-O-Ti, Ti-O-Zr or Zr-O-Zr bonding which could lead to phase separation. The chosen prehydrolysis conditions were TEOS:EtOH:H_2O in the presence of HCl (pH=1), stirring for 30 minutes. The appropriate quantity of $Zr(OPr^n)_4$ and $Ti(OPr_i)_4$, which has been modified with acac and stirred for 30 minutes, was then slowly added to the prehydrolysed TEOS solution while stirring. The stoichiometry of the modified alkoxide precursors were adjusted to achieve a total metal content of between 10 and 20 mol %, with the TiO_2 and ZrO_2 contents both varying between 5 and 15 mol%. The resulting sol was then left to gel; this typically took a few days, depending on composition.

Note that all reagents were loaded in a dry box under a N_2 atmosphere and transferred using syringes to avoid absorption of moisture from the atmosphere. Samples for ^{17}O MAS NMR were prepared using 10 mol% [17]O enriched water (D-chem).

All samples were aged for one week before being air dried for several days, finely ground and then pumped under vacuum for 24 hours to remove any excess solvent. Heat treatments were performed at a heating rate of 2° C min with each temperature maintained for 2 hours. Five samples were prepared with nominal composition of $(TiO_2)_x(ZrO_2)_y(SiO_2)_{1-x-y}$ where (x = 0.05, y = 0.05), (x = 0.05 y = 0.15), (x = 0.10, y = 0.05), (x = 0.10, y = 0.10), (x = 0.15, y = 0.05). Each sample was then divided into four portions, which were either left unheated or heated to 250, 500, or 750° C. [17]O enriched samples were prepared for the compositions (x = 0.15, y = 0.05), (x = 0.05, y = 0.15). These enriched samples were heated differently; first, the sample was heated to 250° C then an NMR spectrum was taken. The same sample was further heated to 500° C and another NMR spectrum was then taken. Finally, the same sample was heated to 750° C and the final NMR spectrum was taken. In addition, in order to prevent the loss of [17]O, heat treatment for [17]O samples was done under an N_2 atmosphere.

3.2 Magic Angle Spinning NMR

^{29}Si NMR spectra of all the ternary xerogels were acquired on a Bruker MSL-300 spectrometer operating at 59.62 MHz using a Bruker 7-mm double bearing probes. The [29]Si spectra were collected using MAS at typically 5 kHz with a 2 μs (~30° tip angle) pulse and a 20 s recycle delay. The pulse delay was sufficient to prevent saturation. Chemical shift values were referenced externally to TMS (δ = 0 ppm) and each spectrum was the result of summing ~1600 scans.

^{17}O NMR spectra of both ^{17}O-enriched xerogels were acquired on Chemagnetics CMX 240 and 360 spectrometers operating at 32.27 and 48.18 MHz, respectively, using a Bruker 4-mm double bearing probes. The ^{17}O MAS spectra was recorded using a spin-echo θ - τ - 2θ pulse sequence with $\theta = 90°$. The τ delay value was determined in MAS experiments by the spinning frequency of the rotor ($R_0 \sim 12$ kHz) and was therefore of 80-85 μs (equivalent to $1/R_0$). The acquisition was not synchronized with the rotor and a recycle delay of between 0.5 and 2 s was employed which gave relaxed spectra with 30000-150000 FIDs added together. Chemical shift values were referenced externally to distilled water ($\delta = 0$ ppm). Recording spectra at different magnetic fields was done to improve confidence in simulating the resonances.

^{1}H NMR spectra of both ^{17}O-enriched xerogels were acquired on Chemagnetics CMX 360 spectrometer operating at 360 MHz, using a Bruker 4-mm double bearing probe. The ^{1}H spectra were collected using MAS at typically 12 kHz with a 4 μs pulse and a 20 s recycle delay. Chemical shift values were referenced externally to TMS ($\delta = 0$ ppm). Each spectrum was the result of summing ~64 FIDs together. Quantitative measurement against adamantane ($C_{10}H_{16}$) was performed.

3.3. Cross Polarisation

^{13}C NMR spectra of $(TiO_2)_{0.05}(ZrO_2)_{0.15}(SiO_2)_{0.80}$ xerogels were acquired on a Bruker MSL-300 spectrometer operating at 76 MHz, using a 7-mm Bruker MAS probe. The ^{13}C spectra were collected using CP MAS at typically 5 kHz with a 7 μs pulse, a 2 s recycle delay and 1 ms contact time. Chemical shift values were referenced externally to adamantane ($\delta_1 = 38.56$ ppm and $\delta_2 = 29.50$ ppm relative to TMS) and each spectrum was the result of adding ~1600 FIDs together.

4. Results and data analysis

4.1. ^{29}Si MAS NMR

The ^{29}Si MAS NMR spectra were deconvolved by Gaussian fitting using WinFit software; three signals could be distinguished at typically -91, -100 and -108 ppm with varying intensities. Each resonance represents a specific degree of Si-O-Si polymerisation. The -91 ppm signal comes from Si sites in a Q^2 configuration, and the -100 and -108 ppm signals come from Q^3 and Q^4, respectively (Q^n stands for a SiO$_4$ unit with n bridging oxygens). The results of the Gaussians fitting are summarised in Table 1 and 2. Figure 2 and 3 show the ^{29}Si NMR data and peak deconvolution for the sample and clearly illustrated a shift to higher average Q species with heat treatment.

Table 1 ^{29}Si NMR data[a] for $(TiO_2)_x(ZrO_2)_y(SiO_2)_{1-x-y}$ xerogels

Sample	Heat Treatment/ °C	Q²			Q³			Q⁴		
		fwhm/Hz	δ/ppm	I (%)	fwhm/Hz	δ/ppm	I (%)	fwhm/Hz	δ/ppm	I (%)
	None	660	-94.1	10.7	400	-100.9	35.8	530	-109.3	53.5
5 mol % of TiO₂	250	570	-92.1	9.9	435	-99.5	27.2	640	-107.9	62.9
5 mol % of ZrO₂	500	860	-94.4	6.2	585	-100.2	19.6	690	-108.7	74.2
	750	0	-92.0	0.0	720	-99.3	15.1	730	-109.2	84.9
	None	830	-94.5	17.6	400	-100.2	32.0	540	-107.7	50.4
5 mol % of TiO₂	250	450	-90.9	6.0	500	-98.9	28.4	660	-107.3	65.6
15 mol % of ZrO₂	500	550	-90.7	5.0	610	-98.8	21.3	760	-108.1	73.7
	750	1120	-90.4	4.4	730	-98.6	13.2	820	-109.2	82.4
	None	580	-94.7	8.7	380	-100.9	32.6	570	-109.0	58.8
10 mol % of TiO₂	250	560	-93.4	8.1	490	-99.7	32.1	610	-107.8	59.8
5 mol % of ZrO₂	500	640	-93.2	7.6	560	-100.6	21.9	660	-109.3	70.5
	750	510	-94.2	2.2	630	-100.6	12.0	750	-110.0	85.8
	None	770	-94.0	13.1	440	-100.4	34.6	580	-108.5	52.2
10 mol % of TiO₂	250	630	-91.3	10.8	500	-99.4	30.2	640	-107.6	58.9
10 mol % of ZrO₂	500	820	-90.8	10.3	640	-100.6	26.3	690	-109.1	63.4
	750	470	-92.1	3.3	550	-98.7	9.5	800	-109.4	87.2
	None	470	-94.9	13.5	340	-100.8	27.7	600	-108.1	58.8
15 mol % of TiO₂	250	780	-90.6	13.0	590	-99.5	25.4	770	-107.9	61.6
5 mol % of ZrO₂	500	630	-91.1	6.2	610	-99.8	20.7	750	-109.0	73.1
	750	820	-91.2	4.7	720	-100.4	11.4	800	-110.6	83.9

[a] fwhm, δ and I represent the line width, ^{29}Si chemical shift and relative intensity, respectively. Errors: fwhm ±25Hz, δ ±1.5ppm, I ±5%.

Table 2 ^{29}Si NMR data[b] for $(TiO_2)_x(ZrO_2)_y(SiO_2)_{1-x-y}$ xerogels (^{17}O- enriched xerogels heated progressively and under N_2)

Sample	Heat Treatment/ °C	Q²			Q³			Q⁴		
		fwhm/Hz	δ/ppm	I (%)	fwhm/Hz	δ/ppm	I (%)	fwhm/Hz	δ/ppm	I (%)
	None	570	-95.0	9.8	410	-100.9	28.7	580	-109.3	61.6
15 mol % of TiO₂	250	690	-94.3	8.1	570	-101.8	24.6	660	-108.9	67.2
5 mol % of ZrO₂	500	630	-90.4	4.3	640	-97.6	13.4	840	-107.3	82.3
	750	540	-90.9	2.4	640	-102.8	12.7	670	-111.1	84.8
	None	830	-95.0	12.6	400	-101.2	33.3	570	-108.1	54.0
5 mol % of TiO₂	250	450	-91.0	8.7	500	-99.1	28.7	680	-107.1	62.6
15 mol % of ZrO₂	500	550	-89.7	4.1	610	-97.5	12.7	840	-106.8	83.2
	750	1120	-89.4	4.1	730	-101.3	11.4	760	-109.9	84.4

[b] fwhm, δ and I represent the line width, ^{29}Si chemical shift and relative intensity, respectively. Errors: fwhm ±25Hz, δ ±1.5ppm, I ±5%.

12
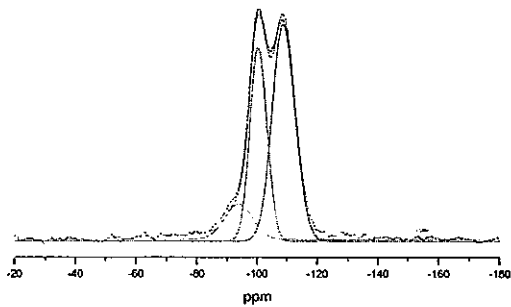
Fig. 2 ^{29}Si MAS NMR spectra showing deconvolution by Gaussian fitting for a $(TiO_2)_{0.10}(ZrO_2)_{0.05}(SiO_2)_{0.80}$ xerogels in the unheated form along with simulation

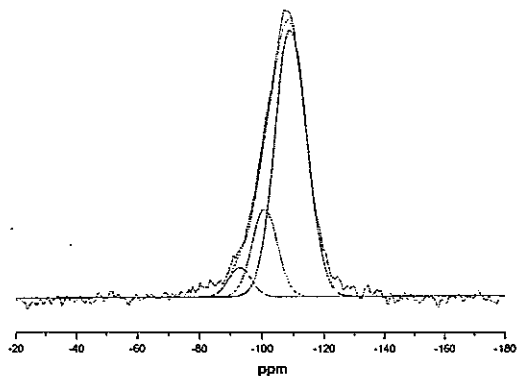**Fig. 3** ^{29}Si MAS NMR spectra showing deconvolution by Gaussian fitting for a $(TiO_2)_{0.10}(ZrO_2)_{0.05}(SiO_2)_{0.80}$ xerogels after heat treatment to 750° C form along with simulation

4.1.2. ^{17}O MAS NMR

The ^{17}O MAS NMR spectra recorded at 5.6 T and 8.45 T are presented in Figure 4 - 7. In the dried, unheated xerogels, the spectra are dominated by a resonance which peaks at close to 0 ppm and shows negative shift due to the quadrupolar interaction [25, 26]. This resonance is due to Si-O-Si bridges [7] with a contribution from Si-OH groups [27]. The signal has spinning sidebands from the MAS process at about 260 and –240 ppm. The resonances between ~100 and ~300 ppm observed for both samples are in good agreement with ^{17}O liquid state study [28] and hence can be assigned to Si-O-Ti and Si-O-Zr bonding respectively. On heating, the spectrum largely remains unchanged after heating up to 500° C apart from the change in the relative intensity. After heating to 750° C there is more
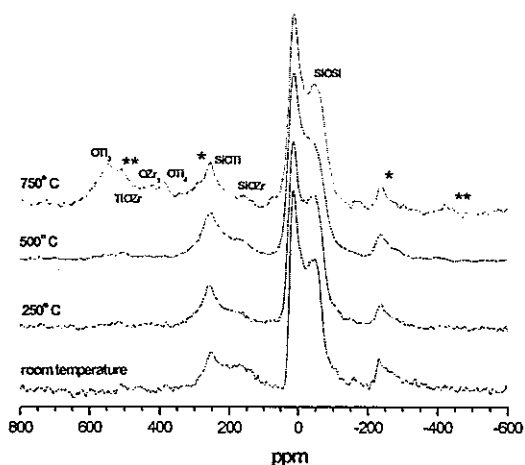

Fig. 4 ^{17}O MAS NMR of a $(TiO_2)_{0.15}(ZrO_2)_{0.05}(SiO_2)_{0.80}$ xerogels at 8.45 T after various heat treatment. Asterisks indicate spinning sidebands.

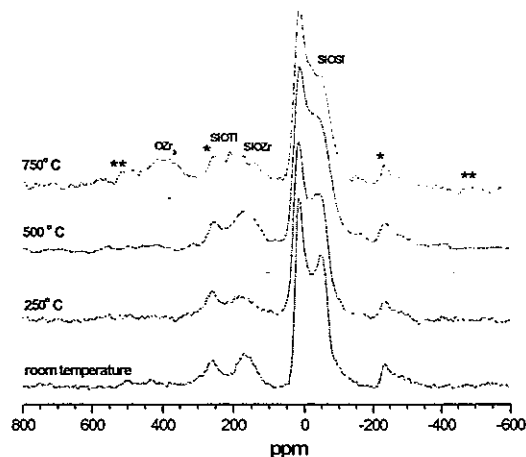**Fig. 5** ^{17}O MAS NMR of a $(TiO_2)_{0.05}(ZrO_2)_{0.15}(SiO_2)_{0.80}$ xerogels at 8.45 T after various heat treatment. Asterisks indicate spinning sidebands.

significant change of the structure. Resonances between ~300 and ~600 ppm were observed for both samples which indicate phase separation [28] of Ti-O-Si and Zr-O-Si bonding to OTi_3, OTi_4, OZr_3 and possibly Ti-O-Zr bonding.
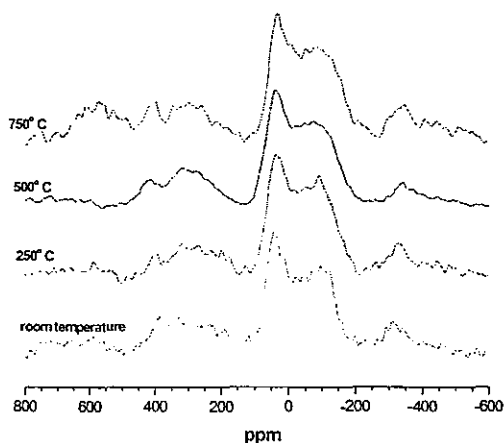

Fig. 6 ^{17}O MAS NMR of a $(TiO_2)_{0.15}(ZrO_2)_{0.05}(SiO_2)_{0.80}$ xerogels at 5.6 T after various heat treatment.
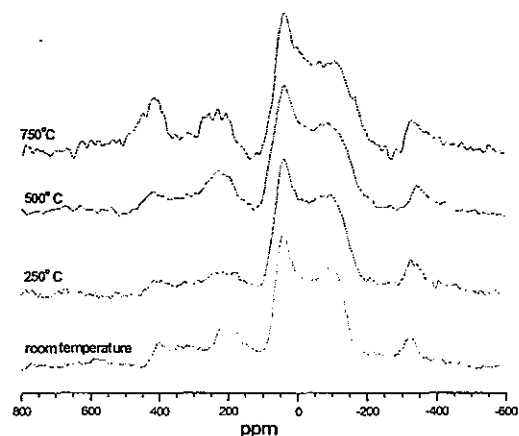
Fig. 7 ^{17}O MAS NMR of a $(TiO_2)_{0.05}(ZrO_2)_{0.15}(SiO_2)_{0.80}$ xerogels at 5.6 T after various heat treatment.

4.1.4. ^{13}C CP MAS NMR

The ^{13}C CP MAS NMR spectra recorded at 7.05 T are presented in Figure 8. In the dried, unheated xerogels, the spectra are dominated by a resonance which peaks between ~5 and ~40 ppm. These resonances can be assigned to C-H_3 bonds. The resonances observed between ~45 and ~115 ppm can be assigned to C-O bonds and resonances observed between ~180 and ~200 ppm can be assigned to C=O bonds [29]. On heating, the spectrum slowly loses its intensity and after heating to 500° C, only resonances between ~120 and ~150 ppm, which can be assigned to C=C bonding, can be observed [29].
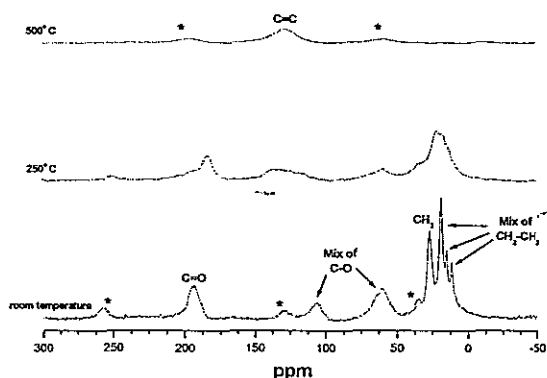
Fig. 8 ^{13}C CP MAS NMR of a $(TiO_2)_{0.05}(ZrO_2)_{0.15}(SiO_2)_{0.80}$ xerogels after various heat treatment. Asterisks indicate spinning sidebands.

4.1.5 ^{1}H MAS NMR

The integrated intensities of ^{1}H spectra were calculated using Spinsight 4.1 software and quantitative measurements, which was run on each separate day ^{1}H spectra were performed, were done by comparing each result with the integrated intensity of a reference adamantane spectrum. The ^{1}H MAS NMR results obtained at 8.45 T are presented in Table 3. It can be seen that the amount of ^{1}H went through a significant decrease as the temperature is increased (the value of ^{1}H at heat treatment of 750° C is virtually zero).

Table 3 Amount of Hydrogen in $(TiO_2)_x(ZrO_2)_y(SiO_2)_{1-x-y}$ Samples as determined by ^{1}H NMR

Sample	Heat Treatment/ °C	Total amount (moles/g)
15 mol % of ZrO2 5 mol % of TiO2	None	2.86×10^{-3}
	250	1.75×10^{-3}
	500	5.05×10^{-4}
	750	2.20×10^{-5}
15 mol % of TiO2 5 mol% of ZrO2	None	2.98×10^{-3}
	250	1.28×10^{-3}
	500	7.75×10^{-4}
	750	7.10×10^{-5}

15

5. Discussion

As can be seen from Table 1 and 2, the ^{29}Si MAS NMR results from TiO_2-ZrO_2-SiO_2 xerogels exhibit a general trend towards more polymerised Q^n species as the temperature of the heat treatment increases. These results are expected, since all the samples are composed predominantly of SiO_2 and it is well known that when a silica sol-gel is heated to progressively higher temperatures, further condensation and the resultant increase in cross-linking leads to an increase in the proportions of higher Q species [25]. Table 1 shows that the extent of condensation of the silica network is of similar trend. For the same composition of xerogels, the results shown in Table 2 show a slight difference after heat treatment of 500° C. There are two possible reasons behind this. First the condition under which the samples are being heated, and secondly, the way they are heated. These differences are also being supported by the EXAFS results, and hence will be further investigated [30].

The ^{17}O MAS NMR results from enriched $(TiO_2)_{0.05}(ZrO_2)_{0.15}(SiO_2)_{0.80}$ and $(TiO_2)_{0.15}(ZrO_2)_{0.05}(SiO_2)_{0.80}$ samples shown in Figure 4-7, yield information on the degree of atomic mixing of the two oxides. All of the spectra show clear resonances due to Si-O-Si (~0 ppm), Ti-O-Si (~150 ppm) and Zr-O-Si (~250 ppm) before being heated up to 750° C. After heat treatment at 750° C, resonances due to phase separation of Ti-O-Si and Zr-O-Si to form OTi_3, OTi_4, OZr_3 and possibly Ti-O-Zr were being observed. This suggests that the environment of the oxygen in the phase-separated part of both ^{17}O-enriched samples contain clusters of titania and zirconia. Despite phase separation, some resonance is still observed at ~150 ppm and ~250 ppm for both samples, indicating that some proportion of the titania and zirconia are atomically mixed with the silica.

Both the ^{13}C and ^{1}H NMR results show that as the temperature is increased, the amount of ^{13}C and ^{1}H is reduced significantly. This is expected, as the samples are heated to high temperature (750° C), both the ^{13}C and ^{1}H would have reacted with air leaving the samples with only a tiny amount of carbon and hydrogen.

6. Future development

The present study has led to an investigation of both the effect and condition of heating which might lead to the occurrence of phase separation. This will be investigated in further detail in the next few months. Moreover, quantitative data analysis of the ^{17}O spectra samples will be performed and a study of Ti NMR and possibly Zr NMR of the present samples will follow this. Alongside the parallel studies carried out at the University of Kent, it was hoped that a model structure for the system would be developed.

In addition to the above study, NMR studies on HfO_2-SiO_2 systems will be performed. This is to follow the results obtained from the EXAFS studied carried out at Daresbury laboratory. Again, the aim would be to produce a model structure for the system.

7. Conclusion

$(TiO_2)_x(ZrO_2)_y(SiO_2)_{1-x-y}$ sol-gel derived glasses has been investigated by ^{29}Si MAS NMR which shows that the extent of condensation of the silica network is similar in almost all the samples. ^{17}O MAS NMR studies of both $(TiO_2)_{0.05}(ZrO_2)_{0.15}(SiO_2)_{0.80}$ and $(TiO_2)_{0.15}(ZrO_2)_{0.05}(SiO_2)_{0.80}$ samples show that phase separation of Ti-O-Si and Zr-O-Si to form OTi_3, OTi_4, Ozr_3 and possibly Ti-O-Zr were being observed after heat treatment at 750° C. Finally, both the ^{13}C and ^1H NMR results show the removal of organics and OH groups as the samples are heat treated.

Acknowledgement

References

[1] P.C. Shultz and H.T. Smyth, *Amorphous Materials*, Edited by Douglas EW and Ellis B (Wiley, London, 1972).

[2] M. Nogami, (1985), *J Non-Cryst.Solids*, **69**, pp 415.

[3] C.J Brinker and G.W. Scherer, (1990), *Sol-Gel Science, The Physics and Chemistry of Sol-Gel Processing*, Academic Press, San Diego.

[4] A. Matsuda, Y. Matsuno, S. Katayama, T. Tsuno, N. Toghe, T. Minami, (1993), *J. Am. Ceram. Soc.*, **76**, pp. 2899

[5] M. Itoh, H. Hattori, and K.J. Tanabe, (1974), *J. Catalyst*, **35**, pp. 225

[6] H. Schröeder, (1969), *Phys. Thin Films*, **5**, pp. 87

[7] M.E. Smith and H.J. Whitfield, (1994), *J. Chem. Soc. Chem. Comm.*, **6**, pp. 723

[8] P.J. Dirken, M.E.Smith and H.J. Whitfield, (1995), *J. Phys. Chem.*, **99**, pp. 395

[9] D.M. Pickup, G. Mountjoy, M. Holland, G.W. Wallidge, R.J. Newport and M.E. Smith, (2000), *J. Mater. Chem.*, **10**, pp 1887

[10]T.J. Bastow, A.F. Moodie, M.E. Smith and H.J Whitfield, (1993), *J. Mater. Chem.*, **3**, pp.697

[11]J-J. Cheng and D-W. Wang, (1988), *J. Non-Cryst. Sol.*, **100**, pp. 288

[12]M. Emili, L. Incoccia, S. Mobilio, G. Fagherazzi and M. Guglielmi, (1985), *J. Non-Cryst. Solids*, **74**, pp. 129

[13]E.R. Andrew, 'Magic Angle Spinning', *Encyclopedia of NMR*, pp. 2891

[14]H. Eckert, (1992). 'Structural characterisation of noncrystalline solids and glasses', *Progress in NMR spectroscopy*, **24**, pp. 173

[15]J.J. Fitzgerald and S.M. De Paul, (1998), *Solid State NMR Spectroscopy of Inorganic Materials*, Chapter 1, pp.19

[16]R.K Harris (1986), *Nuclear Magnetic Resonance Spectroscopy*, Longman

[17]S.R. Hartmann and E.L. Hahn, (1962), *Phys. Rev*, **128**, pp. 2042

[18]F. Babonneau, J. Maquet (2000), *Polyhedron*, **19**, pp. 315

[19]L.W. Kelts, N.J. Armstrong, (1989), *J. Mater. Res.*, **4**, pp.423

[20]J.P. Kintzinger, (1983) in: *NMR of Newly Accessible Nuclei*, vol. 2, Academic Press, pp. 79

[21]T.H. Walter and E.Oldfield, (1989), *J. Phys. Chem.*, **93**, pp. 6744

[22]T.J. Bastow and S.N. Stuart, (1990), *Chem. Phys.*, **143**, pp. 459

[23]B.E. Yoldas, (1986), *J. Mater. Sci.*, **21**, pp. 1086

[24]B.E. Yoldas, (1980), *J. Non-Cryst. Solids*, **38**, pp. 81

[25] D.M. Pickup, G. Mountjoy, M. Holland, G.W. Wallidge, R.J. Newport and M.E. Smith, (2000), *J. Mater. Chem.*, **10**, pp 1887

[26] M.E. Smith, (1993), *Appl. Magn. Reson.*, **4**, pp. 1

[27] T.M. Walter, G.L. Turner and E. Oldfield, (1988), *J. Magn. Reson.*, **76**, pp.106

[28] L. Delattre and F. Babonneau (1997), *Chem. Mater.*, **9**, pp. 2385

[29] I. Poplett, (2001), Private communication, University of Warwick, Coventry, UK

[30] G. Mountjoy, M. Holland, R.J. Newport and M.E. Smith, Private communication